Bioresource Technology 179 (2015) 227–233

Contents lists available at ScienceDirect

Bioresource Technology

journal homepage: www.elsevier.com/locate/biortech

Pyrolysis kinetics of raw and hydrothermally carbonized Karanj (*Pongamia pinnata*) fruit hulls via thermogravimetric analysis

Md. Azharul Islam [a,b], M. Asif [c], B.H. Hameed [a,*]

[a] *School of Chemical Engineering, Engineering Campus, Universiti Sains Malaysia, 14300 Nibong Tebal, Penang, Malaysia*
[b] *Forestry and Wood Technology Discipline, Khulna University, Khulna 9208, Bangladesh*
[c] *Chemical Engineering Department, College of Engineering, King Saud University, P.O. Box 800, Riyadh 11421, Saudi Arabia*

HIGHLIGHTS

- TGA analysis of karanj fruit hulls (KFH) and its hydrochar were investigated.
- KFH decomposed much faster than that KFH–HTC hydrochar.
- An increased heating value and activation energy were observed in hydrochar.
- The decomposition mechanism was mainly controlled by lignin content.

ARTICLE INFO

Article history:
Received 18 October 2014
Received in revised form 27 November 2014
Accepted 28 November 2014
Available online 12 December 2014

Keywords:
Hydrochar
Karanj fruit hulls
Pyrolysis
Thermogravimetric analysis

ABSTRACT

The pyrolysis of karanj fruit hulls (KFH) and karanj fruit hull hydrothermal carbonization (KFH–HTC) hydrochar was thermogravimetrically investigated under a nitrogen environment at 5 °C/min, 10 °C/min, and 20 °C/min. The pyrolysis decomposition of KFH biomass was faster than that of KFH–HTC hydrochar because of the high volatility and fixed carbon of KFH biomass. Weight loss percentage was also affected by the heating rates. The kinetic data were evaluated with the Kissinger–Akahira–Sunose and Flynn–Wall–Ozawa methods. The activation energy values obtained with these two methods were 61.06 and 68.53 kJ/mol for KFH biomass and 130.49 and 135.87 kJ/mol for KFH–HTC hydrochar, respectively. The analysis of kinetic process mechanisms was verified with the Coats–Redfern method. KFH–HTC hydrochar may play a potential role in transforming biomass to energy-rich feedstock for thermochemical applications because of its high heating value, high fixed carbon, and low ash and sulfur contents.

© 2014 Elsevier Ltd. All rights reserved.

1. Introduction

Biomass refers to organic carbonaceous materials, such as wood products, dried vegetation, crop residues, and aquatic plants, which produce stored energy through photosynthesis by using solar energy. This latent energy in biomass is one of the earliest energy sources of humans. In the last two decades, biomass-based energy has been extensively utilized to generate electricity because of the low-cost waste it generates and its indigenous characteristic. Nearly 15% of the world's total energy consumption and as much as 35% of the energy used in developing countries, mostly for cooking and heating, come from biomass (Balat and Ayar, 2005). Woody biomass is popular in both household and industrial applications because of its high calorific value. It also produces less sulfur and greenhouse gases compared with coal-based fossil fuel. However, the major problem associated with woody biomass use is forest denudation, which causes irreversible erosion patterns and thus alters ecosystem structure. Extensive research is underway to determine alternative sources of wood-based biomass, which are not only cheap but produce abundant renewable waste, for energy generation; examples of renewable waste are those from the different waste biomasses (Kamarudin et al., 2013).

Biomass can be converted to valuable energy forms through thermal, biological and mechanical, or physical processes (White et al., 2011). Pyrolysis is the most widely used thermal decomposition process for biomass that occurs in the absence of oxygen; the products of biomass pyrolysis include char, bio-oil, and gases in an array of simultaneous parallel reactions (Demirbas, 2009). The kinetics for thermal decomposition mainly regulates the conversion process of biomass to obtain the desired final energy products. Therefore, accurate kinetic models are imperative to the efficient utilization of particular biomasses and to the competent process design and scaling in real industrial applications for energy gener-

---

* Corresponding author. Tel.: +60 45996422; fax: +60 45941013.
E-mail address: chbassim@usm.my (B.H. Hameed).

http://dx.doi.org/10.1016/j.biortech.2014.11.115
0960-8524/© 2014 Elsevier Ltd. All rights reserved.

ation. Many methods have been used to describe pyrolysis kinetics data, and these can be generally categorized into model-fitting and model-free (isoconversional) methods. Both techniques have advantages and disadvantages that are described in several studies (Slopiecka et al., 2012).

Hydrothermal carbonization (HTC) is a wet pyrolysis biomass process that is used to yield a solid coal-like product, called hydrochar, under mild conditions (Funke and Ziegler, 2010). The physical and chemical properties of hydrochar are different from those of the char produced by dry pyrolysis. HTC usually has a higher solid yield than dry pyrolysis, and it does not need to dry the biomass before pyrolysis unlike traditional dry pyrolysis. The uses of wet biomass to convert energy-dense solid fuels offer new opportunities in the energy sector. HTC char is also nontoxic, whereas its low sulfur content makes the product easy to transport and store. These characteristics inherently overcome some disadvantages of coal. Hydrochar has been successfully used in several applications as a soil ameliorator, adsorbent, catalyst, and ion exchanger, to name a few (Funke and Ziegler, 2010). The detailed reaction mechanisms in the HTC process remain unknown, but hydrolysis, dehydration, decarboxylation, aromatization, and condensation polymerization may be involved (Libra et al., 2011). Chemically, lignocellulosic biomasses are mainly composed of cellulose, hemicellulose, lignin, and some extractives. Hemicellulose is a branched polymer with a low degree of polymerization and is lacking in repeating β-(1–4)-glycosidic bonds; therefore, 90% of hemicellulose is dissolved in a hot and pressurized atmosphere during the hydrothermal process (Reza et al., 2013). Cellulose consists of highly ordered crystalline structures as a result of the strong hydrogen bonds to other cellulose molecules, hemicellulose, and water. Therefore, cellulose is not dissolved under mild conditions of the HTC process. Lignin is a 3D polymer of hydroxyl phenylpropane monomers and has a complex and insoluble structure whose integrity cannot be destroyed under HTC conditions (Zhang et al., 2008).

Karanj (*Pongamia pinnata*) is a medium-sized evergreen forest tree that belongs to the *Leguminosae* family. The tree is native to tropical and temperate areas, including Australia, Bangladesh, China, Florida, India, Japan, and Malaysia. Karanj is a drought-resistant, semi deciduous, and nitrogen-fixing leguminous tree (Bobade and Khyade, 2012). The fruit or pod is approximately1.7–2 cm long, 1.25–1.7 cm wide, and 1.5–2 g heavy (Meher et al., 2009). Karanj oil is one of the potential non edible bio-oils collected from the seeds. The seed contains 27–39% oil, 20–30% protein, and a group of furano-flavonoids constituting 5–6% of the weight of the oil (Bringi, 1987). Large amounts of karanj fruit hull (KFH) waste are generated after the seeds are collected for bio-oil production. This type of waste has no economic importance but can be used as biomass for energy generation.

This study investigates the pyrolysis kinetics of KFH and karanj fruit hull hydrothermal carbonization (KFH–HTC) hydrochar by using thermogravimetric analysis. The literature on the efficacy of using HTC as biomass pretreatment for pyrolysis is scarce. Thermogravimetric analyses were performed at three different heating rates (5 °C/min, 10 °C/min, and 20 °C/min) under a nitrogen atmosphere. Kinetic parameters were determined with the isoconversional Flynne–Wall–Ozawa (FWO), Kissinger–Akahira–Sunose (KAS), and Coats–Redfern methods.

2. Experimental

2.1. Materials

Karanj fruit was collected from the Engineering Campus of Universiti Sains Malaysia, Malaysia, on June 2014. The pod was separated from the seed with a wooden hammer, and then the extracted seedless pods were washed with normal water to remove dirt. The karanj seedpods were dried through open-air sun drying for 3 days and later with an oven at 105 °C for 24 h. The materials were ground to 200 μm to 500 μm particles and were named as KFHs for further experiments.

The hydrochar of KFH was prepared as follows: 5 g of powdered KFH and 100 mL of distilled water were placed in a 200 mL stainless steel hydrothermal reactor. The reactor was sealed and heated at 200 °C for 5 h at 5 °C/min and then cooled down at room temperature. The char was recovered as a solid coal-like residue designated as KFH–HTC hydrochar. The chars were washed several times with double-distilled water, followed by drying in an oven at 105 °C for 24 h. Thereafter, the dried char samples were kept in a plastic container for further pyrolysis study.

2.2. Methods

Proximate analysis was conducted according to ASTM (American Society for Testing and Materials) established methods for moisture content (ASTM E871-82, 2006), ash content (ASTM E1755-01, 2007), volatile matter (ASTM D3175-02, 2005), and fixed carbon (ASTM E870-82, 2013) with the use of PerkinElmer TGA 7. The sample weight was 5 mg, and the N_2 flow rate was 20 mL/min; the heating rate was maintained at 20 °C/min.

CHNS were conducted on a PerkinElmer 2400 Series II CHNS/O Elemental Analyzer and O was estimated by difference. The heating values of the samples were determined with a bomb calorimeter model IKA C 200 according to German standard method (DIN 51900-1, 2000). The cellulose, hemicellulose, lignin, and extractive contents of the samples were determined according to the methods described by Li et al. (2004).

The thermogravimetric experiment involved drying of both samples at 105 °C for 4 h prior to pyrolysis. The results presented were therefore on a dry basis. The pyrolysis process was analyzed with Perkin Elmer TGA 7. The sample weight was approximately 5 mg and placed in a platinum TGA sample holder. The high purity nitrogen (99.999%) gas was used as purge gas through maintaining the flow rate of 80 mL/min. The analysis was performed between 30 °C and 850 °C, and the temperature increase from 30 °C to 110 °C was maintained for 10 min to completely remove the moisture content. Subsequently, the temperature continued to increase up to 850 °C. Three heating rates (i.e., 5 °C/min, 10 °C/min, and 20 °C/min) were used to examine the pyrolysis of biomass.

2.3. Kinetic modeling background

The rate of solid state decomposition reaction can be stated as follows:

$$\frac{d\alpha}{dt} = k(T)f(\alpha) \tag{1}$$

where α is the conversion during combustion, whereas $d\alpha/dt$ represents the rate of conversion over time t. α can be calculated with Eq. (2).

$$\alpha = \frac{m_o - m_t}{m_o - m_e}, \tag{2}$$

where m_o, m_t, and m_e refer to the sample mass at the initial period, time t, and the end, respectively.

$k(T)$ is the reaction rate constant that may be explained by the Arrhenius law as

$$k(T) = A\exp\left(-\frac{E_a}{RT}\right) \tag{3}$$

where E_a is the activation energy of the reaction, A is the pre-exponential factor, R is the universal gas constant, and T is the absolute temperature.

Now, Eq. (1) can be written as

$$\frac{d\alpha}{dt} = A\exp\left(-\frac{E_a}{RT}\right)f(\alpha) \tag{4}$$

If the temperature increases with the constant heating rate β, then $\beta = \frac{dT}{dt} = \frac{dT}{d\alpha} \times \frac{d\alpha}{dt}$. Therefore, Eq. (4) can be re written as follows:

$$\int_o^\alpha \frac{d\alpha}{f(\alpha)} = g(\alpha) = \frac{A}{\beta}\int_o^T \exp^{-E/RT} dT \tag{5}$$

where $g(\alpha)$ is the integral function of conversion.

Therefore, Eq. (5) is the fundamental equation that is followed by all kinetic methods to determine the kinetic parameters during the pyrolysis process.

2.3.1. Kissenger–Akahira–Sunose method

The KAS method (Kissinger, 1957; Akahira and Sunose, 1971) is based on the following expression:

$$\ln\left(\frac{\beta}{T^2}\right) = \ln\left[\frac{AE_a}{Rg(\alpha)}\right] - \frac{E_a}{RT} \tag{6}$$

The plot of $\ln\left(\frac{\beta}{T^2}\right)$ versus $1/T$ produced a straight line from where the slope determines the activation energy E_a.

2.3.2. Flynn–Wall–Ozawa method

The FWO method is an isoconversional method (Ozawa, 1965; Flynn and Wall, 1966) derived from Doyle's approximation (Doyle, 1961). The method is referred to as a "model-free" method. Therefore, the FWO method calculates the activation energy (E_a) without prior knowledge of the reaction mechanism. With Eq. (5), the reaction rate in logarithmic form can be expressed as follows:

$$\ln(\beta) = \ln\left(\frac{AE_a}{Rg(\alpha)}\right) - 5.331 - 1.052\frac{E_a}{R}\frac{1}{T} \tag{7}$$

The slope of plot $\ln(\beta)$ against $1/T$ at different heating rates determines the value of apparent activation energy E_a when α is constant.

2.3.3. Coats–Redfern method

Coats and Redfern (1964) described the thermal decomposition mechanisms for mass loss. This method is a common integral kinetic method used to describe the reaction process during pyrolysis. The Coats–Redfern method is also based on Eq. (5), that is, if $2RT/E_a \rightarrow 0$, then Eq. (5) can be expressed in the following logarithmic way:

$$\ln\frac{g(\alpha)}{T^2} = \ln\frac{AR}{\beta E} - \frac{E_a}{RT} \tag{8}$$

A plot of $\ln[g(\alpha)/T^2]$ against $1/T$ provides a straight line. The activation energy E_a is calculated from the slope, whereas the pre-exponential factor A is intercepted from the plot. The theoretical explanation for the three kinetic mechanisms to calculate the $g(\alpha)$ values is presented in Table 1. The selection of appropriate mechanisms is based on the high determination of the regression coefficient (R^2) value.

Table 1
Theoretical expressions of $g(\alpha)$ to determine kinetic values by coats redfern method (White et al., 2011).

Mechanism	$g(\alpha)$
Reaction order models	
First-order (F1)	$-\ln(1-\alpha)$
Second-order (F2)	$(1-\alpha)-1-1$
Third-order (F3)	$[(1-\alpha)-2-1]/2$
Diffusion models	
One way transport (D1)	α^2
Two way transport (D2)	$[(1-\alpha)\ln(1-\alpha)]+\alpha$
Three way transport Jander (D3)	$[1-(1-\alpha)^{1/3}]^2$
Ginstling–Brounshtein (D4)	$1-(2\alpha/3)-(1-\alpha)^{2/3}$
Geometrical contraction models	
Contracting area (R2)	$[1-(1-\alpha)^{1/2}]$
Contracting volume (R3)	$[1-(1-\alpha)^{1/3}]$

3. Results and discussion

3.1. Characteristics of the biomass and hydrochar samples

The biochemical and physical properties of KFH and KFH–HTC are presented in Table 2. The volatile matter of KFH biomass was 84.16%, but the percentage of volatile matters considerably decreased to 66.63% after HTC. Similar results on the HTC of grape pomace biomass were reported (Pala et al., 2014). The fixed carbon of HTC char was higher than that of raw biomass, a finding indicating that KFH–HTC hydrochar requires a long combustion time. Ash content is one of the most important indicators of combustibility and post combustion cost of energy materials (Sait et al., 2012). The ash content of hydrochar was relatively low (0.84%) compared with that of KFH biomass (5.79%). The high carbon content (71.81%) and the considerably low sulfur content (0.15%) of KFH–HTC also indicate that the quality of energy materials in hydrochar was better than that of the pristine biomass of KFH. Moreover, the improvement in C content after HTC may have occurred because of deoxygenating reactions (Berge et al., 2011). The chemical composition of KFH and KFH–HTC shows that the amount of hemicellulose decreased from 47.28% to 27.99% after HTC, and the lignin content also decreased from 38.62% to 31.11%. A negligible change in cellulose content (0.29%) was observed after the conversion of KFH biomass into hydrochar because of the high degree of crystallinity of the cellulose units. However, the extractive contents significantly increased from 2.37% to 8.09%. This high amount of extractives (mainly polyphenolic polymeric lignin) may be added during the degradation of lignin and subsequently integrated into KFH hydrochar via recondensation mechanisms under subcritical conditions. The high lignin content of KFH–HTC hydrochar makes it a potential energy-dense material that has a higher heating value (HHV) value (19.8 kJ/g) than KFH biomass (16.54 kJ/g). The strong positive correlation between lignin content and the HHV value of a lignocellulosic fuel was also observed by Demirbaş (2001).

3.2. Thermogravimetric analysis

The weight loss and derivative weight loss curves of the KFH biomass and KFH–HTC hydrochar samples at different heating rates under a nitrogen environment are illustrated in Fig. 1. The pyrolysis process of KFH and KFH–HTC showed three distinct zones at different heating rates. In the first zone, moisture evaporation occurred at 20–250 °C and 30–300 °C for KFH and KFH–HTC, respectively. The corresponding heating rates at this zone were 5 °C/min, 10 °C/min, and 20 °C/min, which resulted in 12.3%, 11.29%, and 10.79% weight losses, respectively, for KFH, and 5.19%, 4.88%, and 3.69%, respectively, for KFH–HTC. In the active second zone, the weight loss percentage obtained by the KFH raw biomass was higher than that obtained by KFH–HTC. The cell wall components of the KFH raw materials can be degraded at the temperature range of 250–450 °C. This result indicates that a high heating rate decreases the weight loss percentage. The main chemical components of the cell wall, such as cellulose and lignin for the

Table 2
Proximate and ultimate analysis and chemical composition of KFH and KFH–HTC.

Samples	Proximate analysis (wt.%)				Elemental analysis (wt.%)					Chemical composition				Bulk density (g/cm^3)	HHV (kJ/g)
	Moisture	Volatile	Fixed carbon	Ash	C	H	O	N	S	Cellulose	Hemicellulose	Lignin	Extractives		
KFH	3.71	84.17	6.33	5.79	45.10	6.13	48.41	–	0.36	11.73	47.28	38.62	2.37	0.51	16.54
KFH–HTC	3.03	66.64	29.49	0.84	71.81	3.45	24.60	–	0.15	11.44	27.99	31.11	8.09	0.27	19.80

KFH biomass, quickly devolatilized because hemicellulose is already decomposed during the first stage of pyrolysis. In the third zone, the weight loss percentage of the KFH raw biomass was less than that obtained in the second zone. Hydrochar already underwent different hydrothermal reaction mechanisms under 200 °C at ambient atmospheric pressure. Libra et al. (2011) state that hydrothermal conditions degrade hemicelluloses from 180 °C to 200 °C, most of the lignin from 180 °C to 220 °C, and cellulose at high temperatures. During this process, a portion of some of the weakly bonded amorphous cellulose, hemicellulose, and lignin with all other water soluble extractives and other intermediate products are washed away by water and finally remain as solid hydrochar with strongly bonded cellulose, hemicellulose, and lignin via recondensation reactions. Therefore, the weight loss of KFH–HTC hydrochar in the second zone was less than that in the third zone. Finally, the complete volatilization of the KFH biomass and KFH–HTC hydrochar occurred at 450–650 °C and 410–750 °C, respectively, and contributed to a weight loss of 36.06–23.76% and 53.66–52.98%, respectively, under different heating rates. Fig. 1a illustrates that no weight loss was detected for KFH biomass in the third zone at 5 °C/min, this result indicated that more than 38% of lignin was unprocessed after 450 °C at low heating rate. This may be happen due to greater thermal resistance of lignin structure. At low temperature a considerable portion of low thermal stable functional groups are cleaved from the lignin structure to prevent further decomposition.

The derivative weight loss percentage, which is related to the weight loss percentage (Fig. 1a and c), is shown in Fig. 1(b and d) for both KFH biomass and KFH–HTC hydrochar. Similar observations were made for the weight loss percentage of both KFH biomass and the KFH–HTC hydrochar derivative, except for KFH biomass at 5 °C/min. A large peak and a high peak temperature at high heating rates were observed for both KFH biomass and KFH–HTC hydrochar. Similar observations were also made in the pyrolysis kinetics of raw and hydrothermally carbonized loblolly pine (Yan et al., 2012).

3.3. Kinetic study

In this study, three commonly used isoconversional kinetic methods, which are KAS, FWO, and Coats–Redfern, were used to determine the major kinetic parameter values during the pyrolysis of KFH and KFH–HTC hydrochar samples. Eqs. (6) and (7) are used for the KAS and FWO methods. The linear plots are illustrated in

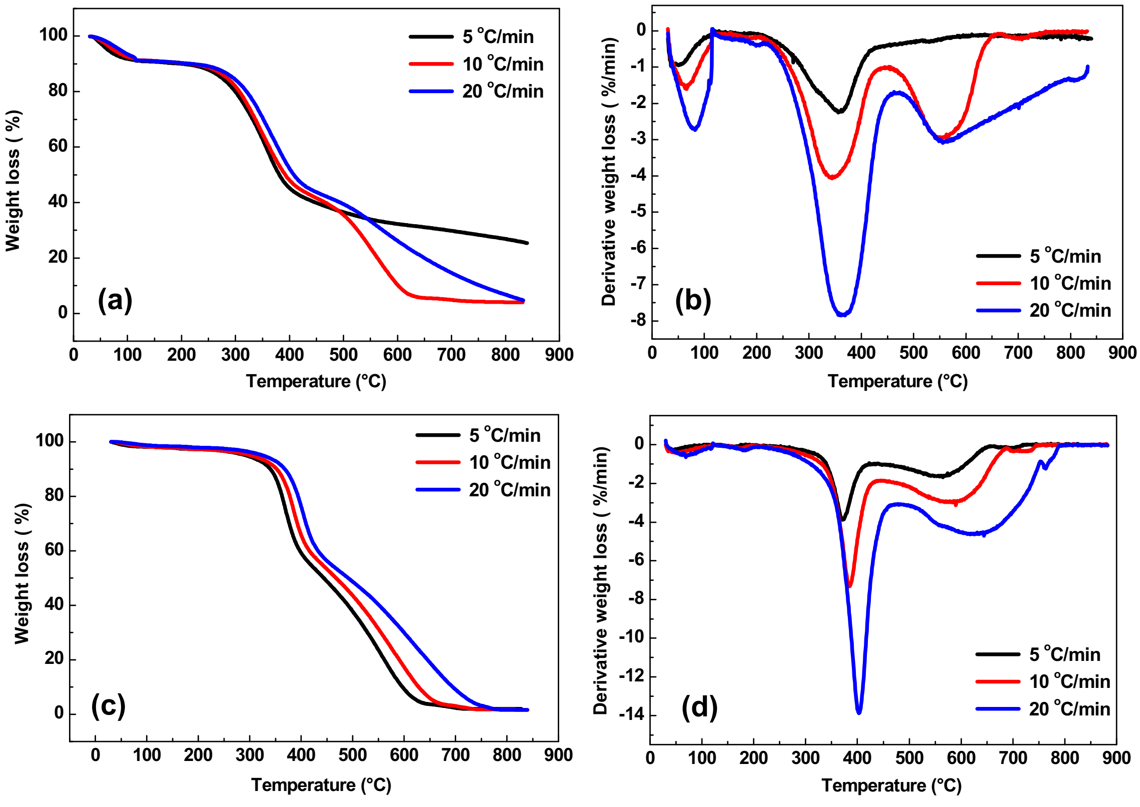

Fig. 1. Effect of heating rates on weight loss (a) KFH biomass, (c) KFH–HTC hydrochar and derivative weight loss of (b) KFH biomass, (d) KFH–HTC hydrochar under N_2.

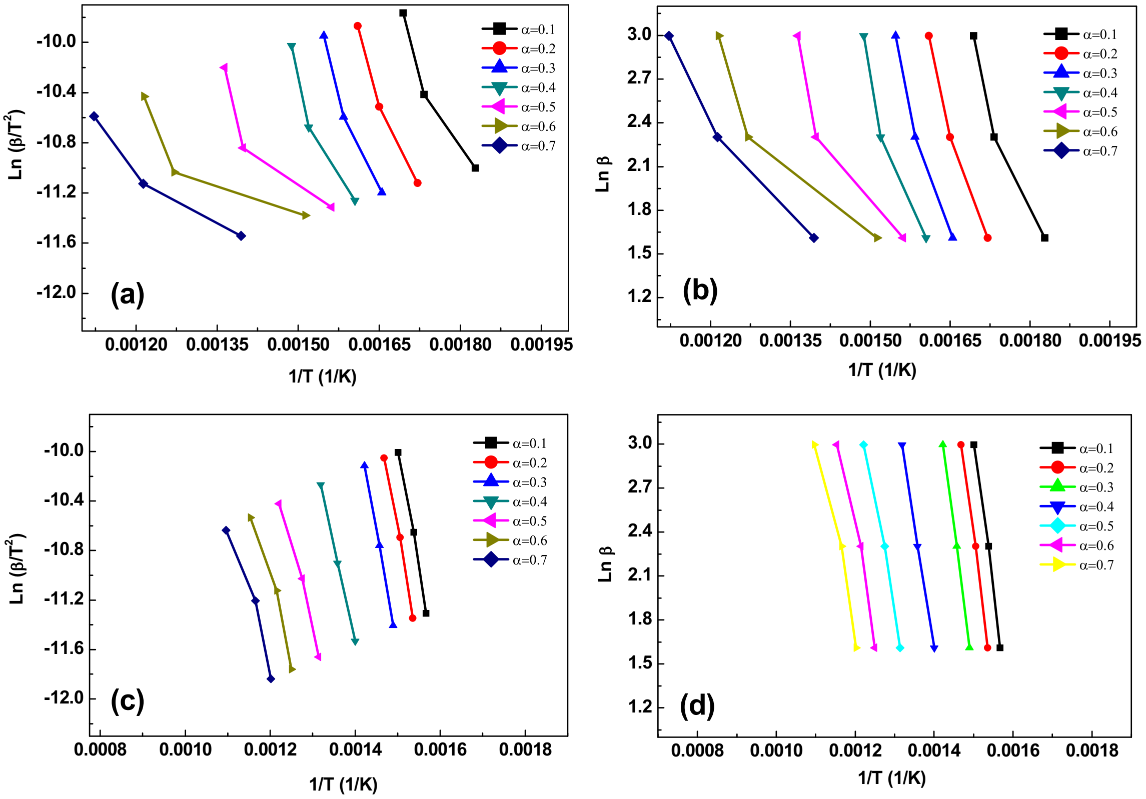

Fig. 2. Isoconversional plots at various conversion degrees (α) for both KFH (up) and KFH–HTC hydrochar (down). (a and c) – KAS method; (b and d) – FWO method.

Table 3
Activation energy and pre-exponential values obtained by KAS and FWO methods.

Samples	α	KAS			FWO		
		E_{KAS} (kJ/mol)	R^2	A (min^{-1})	E_{FWO} (kJ/mol)	R^2	A (min^{-1})
KFH	0.1	72	0.9285	7.72E+04	77.56	0.9428	4.68E+05
	0.2	91	0.9690	3.78E+06	96.34	0.9744	1.63E+07
	0.3	93	0.9608	4.14E+06	98.54	0.9677	1.85E+07
	0.4	81	0.9180	2.84E+05	87.51	0.9344	1.76E+06
	0.5	40	0.8112	4.98E+01	48.40	0.8754	1.28E+03
	0.6	22	0.7669	1.26E+00	32.55	0.8842	9.97E+01
	0.7	28	0.9329	3.92E+00	38.83	0.9650	2.45E+02
	Average	61.06		1.18E+06	68.53		5.29E+06
KFH–HTC	0.1	163	0.9944	4.18E+11	165.52	0.9951	6.94E+11
	0.2	159	0.9952	1.83E+11	161.31	0.9959	3.35E+11
	0.3	158	0.9994	1.12E+11	161.49	0.9995	2.17E+11
	0.4	130	0.9997	1.65E+08	134.78	0.9997	5.39E+08
	0.5	110	0.9876	2.08E+06	116.63	0.9903	1.07E+07
	0.6	103	0.9677	4.02E+05	110.64	0.9751	2.61E+06
	0.7	91	0.9583	5.91E+04	100.74	0.9691	5.17E+05
	Average	130.49		1.02E+11	135.87		1.78E+11

Fig. 2, and their corresponding values calculated from the slopes and intercepts at different degrees of conversion (α) are presented in Table 3. The average activation energy values for KFH biomass with the use of the KAS and FWO methods were 61.06 and 68.53 kJ/mol, respectively, whereas those for KFH–HTC hydrochar with the use of the same methods were 130.49 and 135.87 kJ/mol, respectively. These results indicate that the volatile materials of KFH raw biomass more easily decomposed than the components of the KFH–HTC hydrochar, and the rate of reaction in the former was also faster than that in the latter. In the hydrothermal process, volatile materials evolved from the KFH biomass but did not fully leach out of the reactor, so the majority of the volatile compounds again recondensed and accumulated on the hydrochar with a different reaction mechanism. Yan et al. (2012) also made similar observations on the pyrolysis of raw and hydrothermally treated biomass. Fig. 3 shows the conversion curves with temperature at different heating rates. KFH biomass started to decompose at a lower temperature than the KFH–HTC hydrochar did. Table 3 depicts that the activation energy decreased with an increase in the conversion factor α, but an exception was observed in KFH biomass. Generally, a high activation energy value is considered a barrier to a good biomass. During the initial stages of conversion (see Table 3) in both the KAS and FWO methods, the E_a values were low (72 and 77.56 kJ/mol, respectively, at $\alpha = 0.1$), but these gradually increased to a conversion value α up to a certain limit. This phenomenon is attributed to the quick degradation of the weakly

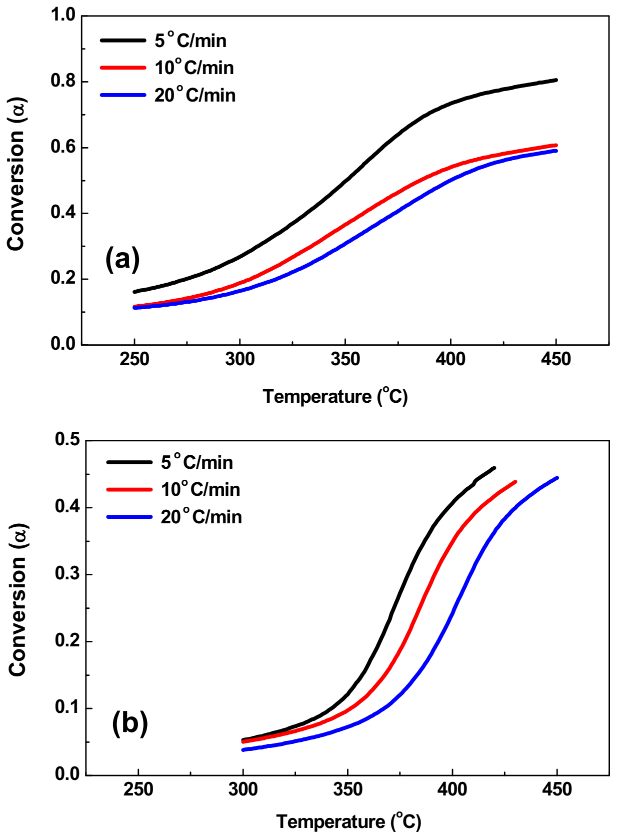

Fig. 3. Extent of conversion curves for the devolatilization process of (a) KFH and (b) KFH–HTC hydrochar at different heating rate.

bonded amorphous cellulose and hemicellulose. After the weak bonds degraded, and then the all-crystalline cellulose also started to degrade, hemicellulose and lignin accounted for the further increase in activation energy (Lopez-Velazquez et al., 2013). Besides, in both samples, lignin content was very high than cellulose content thus, whole pyrolysis was mainly controlled by the lignin and its intermediate products during decomposition. At the beginning with temperature ranges from 100 °C to 200 °C, it was very easy to decompose the KFH sample that resulted low activation energy (less barrier for decomposition) but when lignin starts to degrade at 200 °C onwards, then highly reactive alkyl–aryl–ether bonds are cleaved from the lignin structure. This aryl ether instantly react with other functional groups of lignin intermediates and produce stable higher molecular mass of reaction products through self condensation reactions that are not easily decompose under moderate temperature resulted higher activation energy but at temperature ranges from 650 °C to 750 °C these reaction products decomposed gradually (Brebu and Vasile, 2010). In the KFH–HTC hydrochar sample, this behavior was not observed because of the hydrothermal carbonization process that already degraded the unstructured cellulose and hemicellulose under mild temperature and pressure. The activation energy differs according to the changes in conversional value α and the methods used. Therefore, the decomposition reaction mechanism was not the same, and rather, a multi-step mechanism was involved during the entire process. The complex and heterogeneous nature of the biomass with highly cross-linked cell wall components of cellulose, hemicellulose, and lignin contributed to this outcome, with lignin acting as the main controlling agent. Therefore, identifying the appropriate heat- and mass-transfer mechanisms at different reaction stages is necessary to achieve complete degradation. The activation energy for KFH–HTC was also consistent with the values obtained for the pyrolysis of cellulose (Pasangulapati et al., 2012) and corn straw (Gai et al., 2013).

Table 4
Apparent activation energies and pre-exponential values obtained by Coats-Redfern method.

Samples	Zone	Mechanism	E (kJ/mol)	R^2	A (m^{-1})
KFH	2nd zone	Third-order (F3)	44.09	0.9808	1.4E+01
	3rd zone	Two way transport (D2)	30.10	0.9658	6.0E−02
KFH–HTC	2nd zone	Third-order (F3)	85.57	0.9619	2.0E+04
	3rd zone	Two way transport (D2)	35.89	0.9906	9.7E−02

The Coats–Redfern method for thermogravimetric data was used for the calculation that involved a heating rate of 10 °C/min. Only the best-fitted mechanisms in different zones of the decomposition on the basis of the R^2 value are presented in Table 4. The third-order (F3) mechanism in the second zone and the two-way transport (D2) in the third zone were identified as effective solid state mechanisms for both KFH biomass and KFH–HTC hydrochar. Typically first order and second order reactions are followed during pyrolysis when cellulose content is higher than lignin content in the lignocellulosic biomass (Butterman and Castaldi, 2010) but in this study from Table 2, it was observed that the both samples contained higher lignin amount suggested pyrolytic decomposition was mainly regulated by the lignin and its intermediates. Thus, the complex nature of the lignin and higher thermal resistivity below 500 °C due to various active functional groups in comparison to cellulose, lignin followed the higher reaction order of 3 (Manyà et al., 2003; Butterman and Castaldi, 2010) during pyrolytic degradation. The activation energy values for the KFH and KFH–HTC hydrochar samples in the second zone (44.09 and 85.57 kJ/mol, respectively) were higher than those in the third zone (30.10 and 35.89 kJ/mol, respectively). This result indicates that the second zone was the main critical zone during pyrolysis, where as the third zone was the easiest zone for the degradation of biomass because of physical and mechanical changes that promote high combustibility.

4. Conclusion

The thermogravimetric pyrolysis process of KFH and hydrothermally treated KFH was investigated under a N_2 environment at different heating rates. The KFH–HTC hydrochar had higher heating value, lower ash and sulfur contents than KFH raw biomass. The maximum weight loss of KFH biomass was restricted in the temperature range of 250–450 °C, whereas that of the KFH hydrochar was 410–750 °C. The high lignin content mainly regulated the decomposition mechanisms of both raw biomass and hydrochar. This study suggests that HTC could be an efficient process for biomass conversion to prepare solid energy stock.

Acknowledgements

The first author acknowledges the award of USM-TWAS postdoctoral fellowship in aid for research. The support of Distinguished Scientist Fellowship Program (DSFP) at the King Saud University, Riyadh, Saudi Arabia is greatly appreciated by Prof. M. Asif.

References

Akahira, T., Sunose, T., 1971. Joint convention of four electrical institutes. Sci. Technol. 16, 22–31.
ASTM D3175-02, 2005. Standard Test Method for Volatile Matter in the Analysis Sample of Coal and Coke.

ASTM E1755-01, 2007. Standard Test Method for Ash in Biomass.

ASTM E870-82, 2013. Standard Test Methods for Analysis of Wood Fuels.

ASTM E871-82, 2006. Standard Test Method for Moisture Analysis of Particulate Wood Fuels.

Balat, M., Ayar, G., 2005. Biomass energy in the world, use of biomass and potential trends. Energy Sources 27, 931–940.

Berge, N.D., Ro, K.S., Mao, J., Flora, J.R.V., Chappell, M.A., Bae, S., 2011. Hydrothermal carbonization of municipal waste streams. Environ. Sci. Technol. 45, 5696–5703.

Bobade, S.N., Khyade, V.B., 2012. Detail study on the properties of *Pongamia pinnata* (Karanja) for the production of biofuel. Res. J. Chem. Sci. 2, 16–20.

Brebu, M., Vasile, C., 2010. Thermal degradation of lignin – a review. Cellul. Chem. Technol. 44 (9), 353–363.

Bringi, N.V., 1987. Non-Traditional Oilseeds and Oils in India. Oxford and IBH Publishing Co. Pvt. Ltd., New Delhi, 143–166.

Butterman, H.C., Castaldi, M.J., 2010. Biomass to fuels: impact of reaction medium and heating rate. Environ. Eng. Sci. 27, 539–555.

Coats, A.W., Redfern, J.P., 1964. Kinetic parameters from thermogravimetric data. Nature 201, 68–69.

Demirbaş, A., 2001. Relationships between lignin contents and heating values of biomass. Energy Convers. Manage. 42, 183–188.

Demirbas, M.F., 2009. World biofuel scenario. In: Pandey, A. (Ed.), Handbook of Plant-Based Biofuels. CRC Press, Taylor & Francis Group, Boca Raton, FL, USA, pp. 13–28.

DIN 51900-1, 2000. Testing of solid and liquid fuels – determination of gross calorific value by the bomb calorimeter and calculation of net calorific value – part 1: principles, apparatus, methods. DIN Deutsches Institut für Normung e.V., Berlin, Beuth Verlag GmbH, Germany.

Doyle, C.D., 1961. Kinetic analysis of thermogravimetric data. J. Appl. Polym. Sci. 5, 285–292.

Flynn, J.H., Wall, L.A., 1966. A quick, direct method for the determination of activation energy from thermogravimetric data. Polym. Lett. 4, 323–328.

Funke, A., Ziegler, F., 2010. Hydrothermal carbonization of biomass: a summary and discussion of chemical mechanisms for process engineering. Biofuels Bioprod. Biorefin. 4, 160–177.

Gai, C., Dong, Y., Zhang, T., 2013. The kinetic analysis of the pyrolysis of agricultural residue under non-isothermal conditions. Bioresour. Technol. 127, 298–305.

Kamarudin, S.K., Shamsul, N.S., Ghani, J.A., Chia, S.K., Liew, H.S., Samsudin, A.S., 2013. Production of methanol from biomass waste via pyrolysis. Bioresour. Technol. 129, 463–468.

Kissinger, H.E., 1957. Reaction kinetics in differential thermal analysis. Anal. Chem. 29, 1702–1706.

Li, S., Xu, S., Liu, S., Yang, C., Lu, Q., 2004. Fast pyrolysis of biomass in free-fall reactor for hydrogen-rich gas. Fuel Process. Technol. 85, 1201–1211.

Libra, J.A., Ro, K.S., Kammann, A., Funke, A., Berge, N.D., Neubauer, Y., Titirici, M.M., Fuhner, A., Bens, O., Kern, J., Emmerich, K.H., 2011. Hydrothermal carbonization of biomass residuals: a comparative review of the chemistry, process, and applications of wet and dry pyrolysis. Biofuels 2, 89–124.

Lopez-Velazquez, M.A., Santes, V., Balmaseda, J., Torres-Garcia, E., 2013. Pyrolysis of orange waste: a thermo-kinetic study. J. Anal. Appl. Pyrolysis 99, 170–177.

Manyà, J.J., Velo, E., Puigjaner, L., 2003. Kinetics of biomass pyrolysis: a reformulated three-parallel-reactions model. Ind. Eng. Chem. Res. 42, 434–441.

Meher, L.C., Naik, S.N., Naik, M.K., Dalai, A.K., 2009. Biodiesel production using karanja (*Pongamia pinnata*) and jatropha (*Jatropha curcas*) seed oil. In: Pandey, A. (Ed.), Handbook of Plant-Based Biofuels. CRC Press, Taylor & Francis Group, Boca Raton, FL, USA, pp. 13–28.

Ozawa, T., 1965. A new method of analyzing thermogravimetric data. Bull. Chem. Soc. Jpn. 38, 1881–1886.

Pala, M., Kantarli, I.C., Buyukisik, H.B., Yanik, J., 2014. Hydrothermal carbonization and torrefaction of grape pomace: a comparative evaluation. Bioresour. Technol. 161, 255–262.

Pasangulapati, V., Ramachandriya, K.D., Kumar, A., Wilkins, M.R., Jones, C.L., Huhnke, R.L., 2012. Effects of cellulose, hemicellulose and lignin on thermochemical conversion characteristics of the selected biomass. Bioresour. Technol. 114, 663–669.

Reza, M.T., Yan, W., Uddin, M.H., Lynam, J.G., Hoekman, S.K., Coronella, C.J., Vasquez, V.R., 2013. Reaction kinetics of hydrothermal carbonization of loblolly pine. Bioresour. Technol. 139, 161–169.

Sait, H.H., Hussain, A., Salema, A.A., Ani, F.N., 2012. Pyrolysis and combustion kinetics of date palm biomass using thermogravimetric analysis. Bioresour. Technol. 118, 382–389.

Slopiecka, K., Bartocci, P., Fantozzi, F., 2012. Thermogravimetric analysis and kinetic study of poplar wood pyrolysis. Appl. Energy 97, 491–497.

Yan, W., Islam, S., Coronella, C.J., Vásquez, V.R., 2012. Pyrolysis kinetics of raw/hydrothermally carbonized lignocellulosic biomass. Environ. Prog. Sustainable Energy 31, 200–204.

White, J.E., Catall, W.J., Legendre, B.L., 2011. Biomass pyrolysis kinetics: a comparative critical review with relevant agricultural residue case studies. J. Anal. Appl. Pyrolysis 91, 1–33.

Zhang, B., Huang, H., Ramaswamy, S., 2008. Reaction kinetics of the hydrothermal treatment of lignin. Appl. Biochem. Bioethanol 147, 119–131.